

Using fluorescence quenching of single walled carbon nanotubes with metal ions as a probe of surfactant · · · SWNT interactions

Jonathan J. Brege and Andrew R. Barron*

Richard E. Smalley Institute for Nanoscale Science and Technology, Departments of Chemistry, and Mechanical Engineering, Rice University, Houston, TX, USA

Abstract. The treatment of SDS-SWNTs with the Group 2 metal ions Mg^{2+} , Ca^{2+} , Sr^{2+} , and Ba^{2+} causes quenching of the SWNT's fluorescence in the same manner but to a lesser extent (lower K_{sv}) as they quench SDBS surfacted nanotubes. In contrast, the quenching with the Group 12 metal ions Zn^{2+} , Cd^{2+} and Hg^{2+} does not follow a simple Stern-Volmer behavior. Instead, two effects are observed. First, the different chirality nanotube's emission wavelengths are shifted by all Group 12 metals but to varying degrees. Second, the corrected decreases in fluorescence intensity is only affected above a critical concentration of metal ion, $[M^{2+}]_c$, at which there is a steep change in fluorescence intensity, then above this concentration there is no significant further reduction in fluorescence intensity. There is a distinct relationship between the identity of the metal ion and the critical concentration: $[Zn^{2+}]_c > [Cd^{2+}]_c > [Hg^{2+}]_c$. The differentiation between SDBS- and SDS-surfacted SWNTs can be rationalized by a consideration of the relative hardness of the metal ions and the sulfonate and sulfate "ligands", in particular, the structure of the SDS-SWNT conjugate is overcome by the addition of the Group 12 metal but not by Group 2 metals.

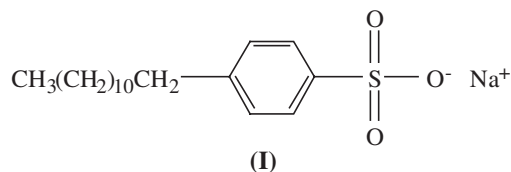
Keywords: Single walled carbon nanotube, Group 2, Group 12, surfactant, fluorescence

1. Introduction

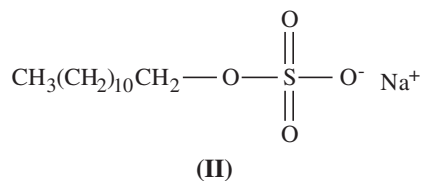
We have previously reported the effect of various metal ions on the fluorescence of sodium dodecylbenzene sulfonate (SDBS, I) surfacted single walled carbon nanotubes (SWNTs). The efficiency of quenching for Group 2 and Group 12 metal ions depends on the identity of the metal ion, the counter ion, and SWNT chirality [1]. In contrast, the transition metal ions Ni^{2+} , Co^{2+} , and Cu^{2+} , exhibit increased quenching compared to the Group 2 and Group 12 analogs. We have assigned this difference to a greater interaction between the metal ions and the surfactant head group for the transition metals as compared to the Group 2 and 12 metal ions [2]. This suggests that the identity of the surfactant could also play a role

*Corresponding author: Andrew R. Barron, Richard E. Smalley Institute for Nanoscale Science and Technology, Rice University, Houston, TX 77005, USA. E-mail: arb@rice.edu.

in defining the extent of metal ion quenching of SWNTs. We are thus interested in comparing the effects of surfactant on the efficacy of metal ion fluorescence quenching of SWNTs.



Previous studies in our group have shown similarities as well as intriguing differences between the quenching of surfactated SWNTs with SDBS and sodium dodecyl sulfate (SDS, II). While coating SWNTs with CdS, it was observed that the fluorescence of SDS-surfactated SWNTs was quenched upon the addition of $\text{Cd}^{2+}/\text{NH}_4\text{OH}/\text{TEA}$ prior to the addition of the sulfur source (thiourea) [3]. Upon addition of thiourea, and the formation of CdS coatings, the fluorescence returned to its original intensity. Thus, it would appear that Cd^{2+} quenches the SDS-SWNT fluorescence, and it is regained when the thiourea removes Cd^{2+} . This is much like our fluorescence quenching of SDBS-SWNTs by Group 2 metal ions, where the fluorescence is regained when EDTA treatment removes the metal ions from the vicinity of the nanotube [1, 2]. While this study suggests SDS behaves the same as SDBS during metal ion quenching, it was noted that there also seemed to be selectivity in that some peaks appeared to be quenched significantly more than others. Other than reporting this observation, no attempt was made to determine its basis. It is clear, therefore, that a comprehensive study to determine the exact role of the surfactant identity in metal quenching of SWNTs is lacking.



Carbon nanotubes have been dispersed in a wide variety of surfactants for different applications [4]. Cationic and anionic surfactants provide good dispersibility and a long shelf life for individualizing SWNTs, making them attractive precursors for SWNT based sensors. Regardless whether the surfactant head group is positive or negatively charged, it is reasonable to propose that ionic surfactants disperse nanotubes in the same way, i.e., the hydrophobic tail adsorbs onto the highly hydrophobic surface of the nanotube and the hydrophilic charged head group extends into the water. The hydrophilic termini are often depicted as forming a layer around the SWNT [5]; however, the exact structure of the surfactant layer is unclear. It is reasonable to assume that each nanotube that is wrapped in surfactant electrostatically repels other similar nanotubes and thus prevents bundling. Certainly the presence of a charged surface is known to debundle SWNTs in solution [6–8] and it is within reason to assume a similar effect is prevalent with charged surfactants.

The anionic surfactants SDS and SDBS should both attract metal ions in a similar manner given the sulfate end group, however, does the structure of the surfactant hydrophobic tail have an indirect effect of the quenching of SWNTs by metal ions? The presence of the benzene in SDBS should provide a strong hydrophobic π -stacking interaction that will not be present for the SDS · · · SWNT conjugate; the structure of the surfactant layer should be distinct. Based upon our previous results [1, 2] it should be possible to observe this phenomenon through fluorescence experiments.

2. Experimental

All chemicals were obtained commercially and used without further purification. All solutions used contained ultra pure (UP) water from a Millipore Milli-Q UV water filtration system. HiPco SWNTs (batch 162.10) were obtained from the Carbon Nanotube Laboratory (Rice University, Houston, TX). Metal salts used were HgCl_2 (EM Science), BaCl_2 (Merck), $\text{Hg}(\text{OAc})_2$ and MgCl_2 (J.T. Baker Chemical Company), CdCl_2 , $\text{Cd}(\text{SO}_4)$, $\text{Cd}(\text{OAc})_2$, $\text{Ca}(\text{OAc})_2$, and $\text{Zn}(\text{SO}_4) \cdot 7(\text{H}_2\text{O})$ (Sigma-Aldrich), and $\text{Ba}(\text{OAc})_2$, CaCl_2 , $\text{Mg}(\text{SO}_4)$, $\text{Mg}(\text{OAc})_2$, and SrCl_2 (Fisher Scientific Company). Sodium dodecyl sulfate (SDS) was obtained from Sigma-Aldrich and used as received. Fluorescence spectra were collected on a NanoSpectralyzer (Applied NanoFluorescence, LLC) with 660 and 785 nm excitation sources, Raman data was obtained using a Kaiser Process Raman spectrometer (Kaiser Optical Inc.) with 785 nm excitation. Absorption spectra were collected on a Varian Cary 400 spectrophotometer. All measurements were taken at room temperature (298 K). Photoluminescence data was collected using a J-Y Spex Fluorolog 3-211 spectrofluorometer equipped with a liquid N_2 -cooled InGaAs detector. All emission intensities were corrected for the wavelength dependencies of the instrument's excitation and detection systems.

2.1. Preparation of surfacted nanotubes

Solutions of SDS surfacted SWNTs (SDS-SWNTs) were prepared by scaling previously published procedures [1, 2, 9]. Raw HiPco SWNTs were dispersed in SDS solution (225 mL, 1%) and sonicated for 15 minutes in a cup-horn sonicator (Cole Palmer CPX-600, 540 W). The solution was centrifuged (Sovall 100S Discovery Ultracentrifuge with Surespin 630 swing bucket rotor) for 4 hours at 122,000 G. The top 2/3 of the solution (surfacted SWNTs) was decanted off and diluted with 1% surfactant solution.

2.2. Fluorescence quenching of surfacted nanotubes

NH_4OH was added to the surfacted tubes and stirred for 24 hours [1, 2]. The $\text{NH}_4\text{OH}/\text{SDS-SWNTs}$ were placed in a cuvette (2.8 mL) and 0.4 mL of metal solution (concentration varying from 0 to 40 mM in 4 mM increments) was added. The solution was inverted several times to induce mixing. After 1 hr, fluorescence measurements were obtained by 660 and 785 nm excitation and absorption spectra were collected. The pH of each $\text{NH}_4\text{OH}/\text{SDS-SWNT}/\text{M}^{n+}$ combination was obtained using pH-indicator strips to ensure that the pH had not changed by more than 0.5 pH units. Each solution was centrifuged at 14,500 rpm for 15 minutes. Fluorescence and absorbance measurements were taken on the supernatant. Final metal concentrations were determined by ICP-AES. Fluorescence spectra were automatically fitted with ANF NanoSpectralyzer software, the 15 most intense peaks were chosen for analysis through Stern-Volmer plots. Fluorescence quenching processes are described by the Stern-Volmer equation ($I_o/I = K_{sv}[Q] + 1$), where $K_{sv} = k_q \tau_o$, K_{sv} is the Stern-Volmer (SV) quenching constant, k_q is the quenching rate constant ($\text{M}^{-1}\text{sec}^{-1}$), and τ_o is the excited singlet lifetime of the fluorophore in the absence of a quencher.

2.3. Raman monitoring

The fluorescence of $\text{NH}_4\text{OH}/\text{SDS-SWNTs}$ with the metal ion solutions was monitored over time using Raman spectroscopy [1, 2]. The $\text{NH}_4\text{OH}/\text{SDS-SWNTs}$ (2.1 mL, 1 : 0.4) were placed in a cuvette. While stirring, in-situ Raman measurements were taken every 45 s (1 second exposure, 5 accumulations). After 5 minutes, the appropriate metal solution (0.3 mL, 20 mM) was added to the cuvette and the spectra were collected for 6 hrs. Changes in electron density in the SWNTs were monitored using Raman spectroscopy.

A similar procedure was employed to monitor the electron density as metal ions were “removed” from solution. The $\text{NH}_4\text{OH}/\text{SDS-SWNT}$'s (2.1 mL, 1 : 0.4) were placed in a cuvette. While stirring, in-situ Raman measurements were taken every 45 s (with 1 s exposure, 5 accumulations). After five minutes, the metal solution (0.3 mL, 20 mM) was added to the cuvette and spectra were collected for 30 minutes. The EDTA solution (0.3 mL, 100 mM in 1 M NH_4OH) was added and spectra were taken for five additional minutes.

3. Results and discussion

Our prior studies focused on the quenching of SDBS surfacted nanotubes by various metal ions, which exhibit Stern-Volmer behavior [1, 2]. This allowed for a quantitative assessment of the quenching and assignment of a mechanism as a basis of comparison for other surfactant systems. To understand the role of the surfactant in fluorescence quenching, we varied the surfactant molecules while keeping the fluorophore (SWNT) and quencher (metal ion) constant.

3.1. Group 2 metals

The treatment of SDS-SWNTs with the Group 2 metal ions Mg^{2+} , Ca^{2+} , Sr^{2+} , and Ba^{2+} causes quenching of the SWNT's fluorescence. A representative plot is shown in Fig. 1. A comparison of the data for the chloride salts (thus eliminating counter ion effects) for the quenching of a particular n,m SWNT (Table 1) shows that within the Group 2 metals the quenching efficiency follows the trend of increasing atomic number (i.e., $\text{Mg} < \text{Ca} \ll \text{Sr} < \text{Ba}$). In this regard, the Group 2 metal ions quench SDS surfacted nanotubes in the same manner as they quench SDBS surfacted nanotubes [1]; all n,m nanotubes are quenched to varying degrees and no spectral shifts occur. This type of behavior is consistent with the SDBS-SWNT with Group 2 metal ion system studied previously [1] and the extent of quenching can be quantified. Table 1 lists the calculated Stern-Volmer quenching constants for all the Group 2 metal ions with SDS and SDBS surfacted nanotubes.

The presence of M^{2+} in solution can effect the loss of surfactant from the nanotube surface in a number of ways because it effects relevant equilibrium processes including how M^{2+} affects solubility

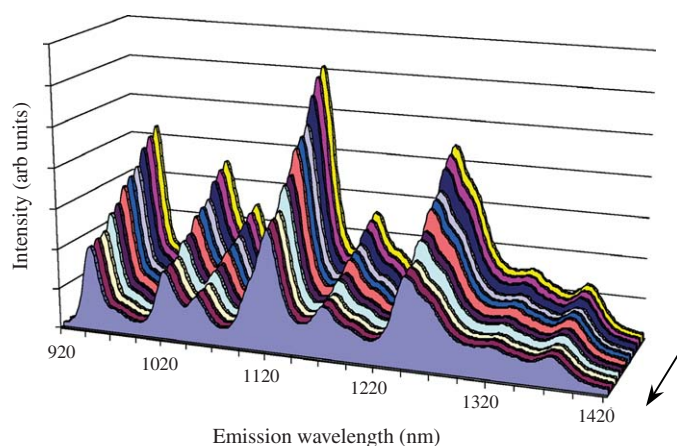


Fig. 1. Decay graph of SDS-SWNTs excited at 660 nm treated with BaCl_2 from 0 to 5.0 mM in 0.5 mM increments. The arrows indicate increasing Ba^{2+} ion concentration.

Table 1

Calculated quenching constants for Group 2 metal complexes with SDBS-SWNTs and SDS-SWNTs from 660 nm irradiation (values for SDS-SWNTs given in parenthesis)

Complex	SWNT n.m															
	10,6	12,4	9,7	13,2	14,0	8,7	10,5	9,5	8,6	7,6	8,4	9,4	10,2	7,5	6,5	8,3
MgCl ₂	a	21	a	11	19	30	27	6	24	31	35	26	28	31	a	30
	a	(10)	a	a	(12)	(7)	(5)	a	(6)	(5)	a	(8)	(10)	(1)	a	(6)
MgSO ₄	a	22	a	22	18	21	21	14	30	43	20	26	33	38	a	36
	a	(7)	a	(4)	(7)	(6)	(5)	(2)	(8)	(9)	a	(15)	(16)	(7)	a	(15)
Mg(OAc) ₂	a	37	a	34	33	27	33	32	43	54	34	42	47	50	a	54
	a	(12)	a	(3)	(6)	(5)	(4)	(1)	(8)	(8)	a	(11)	(13)	(4)	a	(12)
CaCl ₂	9	24	40	40	13	32	41	26	43	61	26	39	43	51	48	51
	a	(177)	(113)	(87)	(231)	(206)	(220)	(21)	(54)	(69)	(47)	(37)	(73)	(60)	(85)	(57)
Ca(OAc) ₂	58	31	67	30	19	55	61	19	43	51	53	39	39	46	46	44
	a	(186)	(109)	(92)	(253)	(217)	(192)	(27)	(63)	(83)	(51)	(42)	(82)	(71)	(101)	(66)
SrCl ₂	138	228	203	295	244	211	224	258	313	377	293	385	382	398	402	392
	(229)	(225)	(216)	(240)	(225)	(275)	(168))	(180)	(227)	(261)	(279)	(216)	(251)	(246)	(270)	(217)
BaCl ₂	222	324	323	460	363	294	361	431	481	611	464	603	596	637	613	640
	(194)	(179)	(192)	(223)	(151)	(197)	(195)	(200)	(208)	(227)	(241)	(236)	(234)	(223)	(202)	(216)
Ba(OAc) ₂	224	386	352	577	413	344	385	508	568	661	483	683	669	710	688	688
	(381)	(215)	(269)	(248)	(225)	(256)	(258)	(238)	(247)	(264)	(310)	(281)	(280)	(266)	(240)	(255)

a, Reliable quenching constants could not be obtained due to low peak intensities.

and packing density of free surfactant in solution micelles. For example, we have previously shown that there occurs a well-characterized association of transition metal ions with SDBS surfactant to form aggregated micelles separate from the SWNTs [2]. Given this observation, we wanted to ensure that the main group ions are not simply removing the surfactant from the nanotube causing a reduction of the fluorescence intensity through bundling or changes in the SWNT solubility and surfactant coverage. For this to occur, the $M^{2+} \cdot \cdot \cdot$ surfactant interaction must be greater than the SWNT $\cdot \cdot \cdot$ surfactant interaction. McDonald et al. found the desorption activation energy for SDBS surfacted tubes to range between 84.3 and 148.8 kJ.mol⁻¹ while SDS surfacted tubes range between 54.8 and 166.8 kJ.mol⁻¹ [10]. Indirect quenching by surfactant removal would predict that SDS tubes would be more greatly affected than SDBS tubes through this mechanism. We do not observe this trend confirming that the $M^{2+} \cdot \cdot \cdot$ SWNT interaction is the controlling factor in the quenching (Table 1) and not the SWNT $\cdot \cdot \cdot$ surfactant interaction. Quenching interactions are limited by the ability of metal ions to come in close proximity of the SWNT surface. While it may be tempting to envision a surfacted SWNT as a cylindrical micelle with a nanotube core [5], a random adsorption of surfactant molecules on the nanotube surface is the more realistic model [11], although there has been experimental evidence for a “grease spot” type distribution of small aggregated micelles [12, 13].

A comparison of the quenching by a particular metal salt (Ba(OAc)₂, BaCl₂, or SrCl₂) reveals that SDS-surfacted nanotubes are generally quenched to a lesser extent (lower K_{sv}) than the SDBS-surfacted nanotubes. This is apparent in Fig. 2 (as well in the comparison of the data in Table 1). For Ba²⁺ and Sr²⁺ for a constant metal ion and nanotube n,m value, K_{sv} SDBS > K_{sv} SDS. The values for Mg²⁺ are all low (Table 1) and hence it is difficult to make a clear comparison, however, it appears to behave in the same manner to that of Ba²⁺ and Sr²⁺. In contrast, for Ca²⁺ the value K_{sv} SDBS ≤ K_{sv} SDS (Table 1).

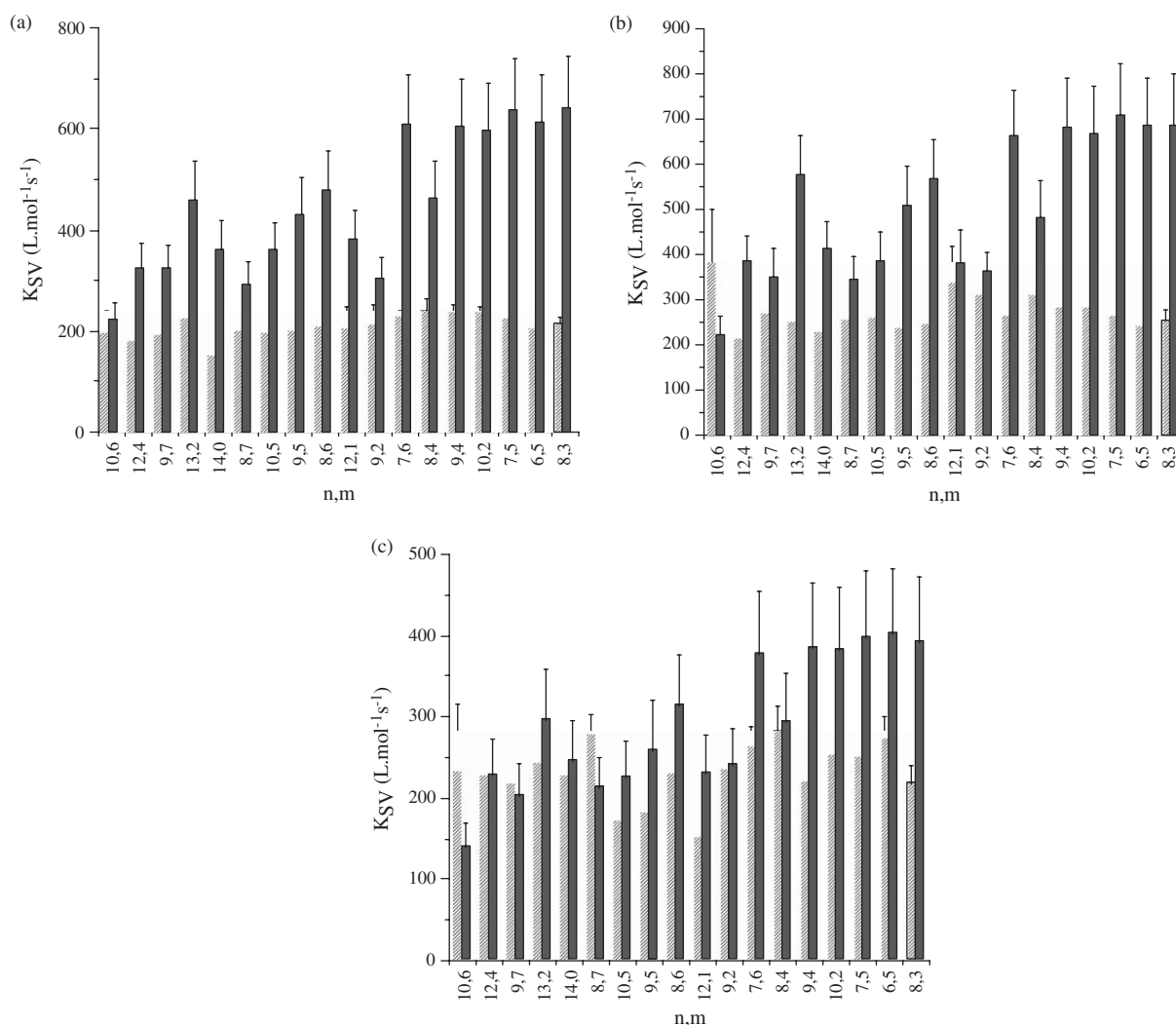


Fig 2. SDS-SWNTs (▨) and SDBS-SWNTs (■) quenched by (a) BaCl_2 , (b) Ba(OAc)_2 , and (c) SrCl_2 .

A surfactant desorption model [14] would predict that $K_{sv} \text{ SDS} > K_{sv} \text{ SDBS}$ because the E_a of surfactant desorption is greater for SDBS than SDS. This is clearly observed for Ca^{2+} , but it is not observed for Ba^{2+} and Sr^{2+} (and possibly for Mg^{2+}); thus, for the latter metals the extent of fluorescence must be due to the accessibility of the metal ion to the SWNT surface rather than surfactant desorption.

The head groups of both surfactants are the same, resulting in similar interactions with the metal ions, i.e., $\text{M}^{2+} \cdots \text{O}=\text{S}(\text{O})_2\text{-R}$. However, the tails of the two surfactants have the potential to act in a slightly different manner. The interaction of the hydrocarbon tail of SDS with a SWNT is limited to van der Waal interactions, and as such, the hydrocarbon tail would randomly adsorb onto the nanotube surface with no preferred orientation. Furthermore, it is reasonable to expect the hydrophilic anionic sulfate group will be oriented away from the hydrophobic SWNT surface (Fig. 3). Thus, the metal ions are also randomly distributed along the nanotube as individual charges. In addition to the same $\text{C}_{12}\text{H}_{25}$ hydrocarbon tail, SDBS has a benzene group that will bind more strongly with the nanotube due to

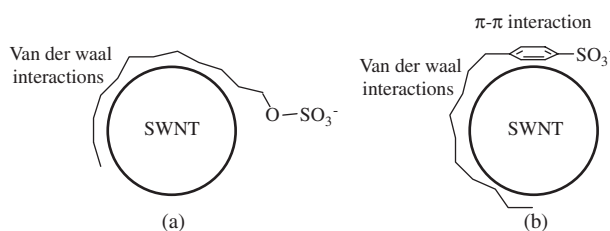


Fig. 3. Schematic of the possible interactions of (a) SDS and (b) SDBS with an individual SWNT.

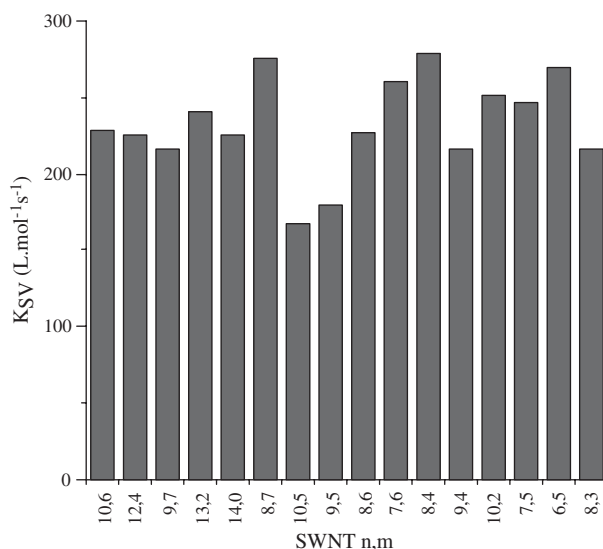


Fig. 4. Stern-Volmer quenching constants for SBS-SWNTs (using 660 nm excitation) as a function of SWNT n,m value in the presence of SrCl₂.

π - π stacking interactions, which stabilizes the surfactant on the nanotube [15]. If a strong π - π stacking interaction is present, the sulfate group, and hence the metal ion, will be closer to the SWNT surface (Fig. 3). Given the quenching effect per metal ion is dependant on the M^{2+} · · · SWNT distance, the extra π - π stacking will result in the metal ion being forced closer to the surface of the SWNT, and therefore a greater quenching being observed per metal ion. This is in-line with the observed fluorescence quenching results for Ba²⁺ and Sr²⁺ (Fig. 2). The opposite effects observed for Ca²⁺ (i.e., K_{sv} SDS > K_{sv} SDBS) suggest that the interaction of Ca²⁺ with SDS is sufficiently strong that surfactant desorption is the dominant mechanism.

We have previously observed for SDBS-SWNTs that a linear correlation exists between the quenching constants and the band gap (and SWNT diameter) [1]: SWNTs with larger band gaps are quenched more efficiently than those with small band gaps. Figure 4 shows the Stern-Volmer quenching constants for SDBS-SWNTs as a function of SWNT n,m value in the presence of SrCl₂. It is clear that there is a dependence of quenching on the identity of the SWNT (i.e., the n,m value). However, unlike the SDBS-SWNT system, no correlation exists, although the variation between SWNTs of particular n,m values does depend on the relative ability of the metal as a quencher.

3.2. Group 12 metals

After investigating the differences between the Group 2 metal ion quenching of SDS and SDBS-SWNT fluorescence, we went on to look at how Group 12 metal ions differentiate between the two anionic surfactants. Our previous results showed that for SDBS-SWNTs, Group 2 and 12 metals both follow Stern-Volmer behavior [1]. Given the similar behavior between Group 2 and 12 metals for SDBS-SWNTs, it would be reasonable to propose that the quenching constant (K_{sv}) for Group 12 quenched SDS-SWNTs should be less than observed for their SDBS counterparts. Surprisingly, a very different scenario is observed. As may be seen from Fig. 5, the quenching of SDS-SWNTs by Cd^{2+} does not follow a simple Stern-Volmer behavior. It appears that some tubes are quenched to a great extent while others are barely affected, as can be observed in the overlay plot in Fig. 6. The same type of decay occurs for both Zn^{2+} and Hg^{2+} . It has been shown that the fluorescence spectra may be fitted for the contributions from each particular n,m SWNT. Each individual spectrum was therefore fitted to determine the intensity

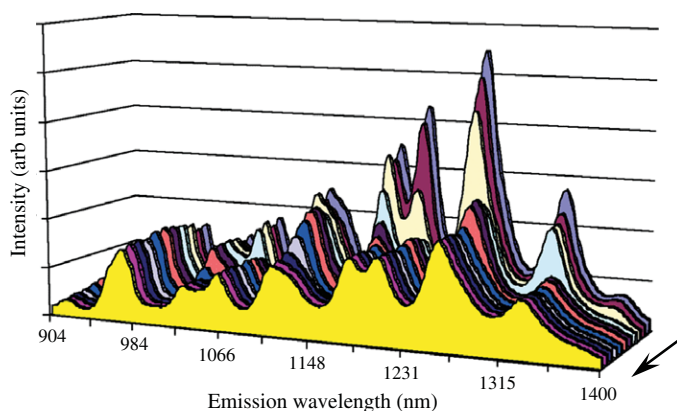


Fig. 5. Decay graph of SDS-SWNTs excited at 785 nm treated and with $CdCl_2$ from 0 to 5.0 mM in 0.5 mM increments. The arrow indicates increasing M^{2+} concentration.

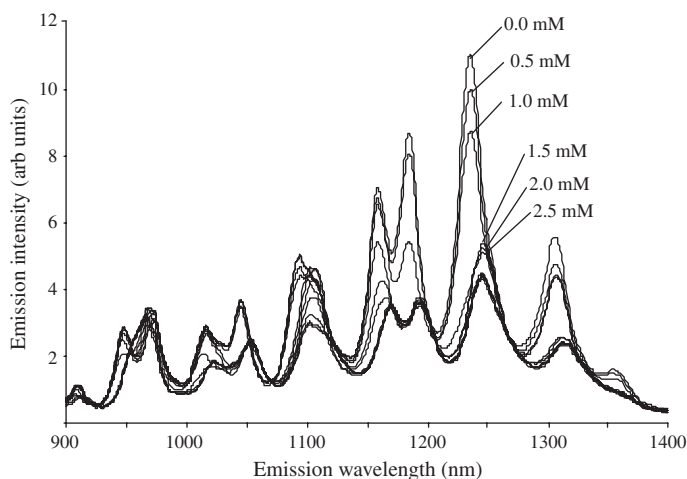


Fig. 6. Overlay plot of SDS-SWNTs excited at 785 nm and treated with $CdCl_2$ from 0 to 5.0 mM in 0.5 mM increments.

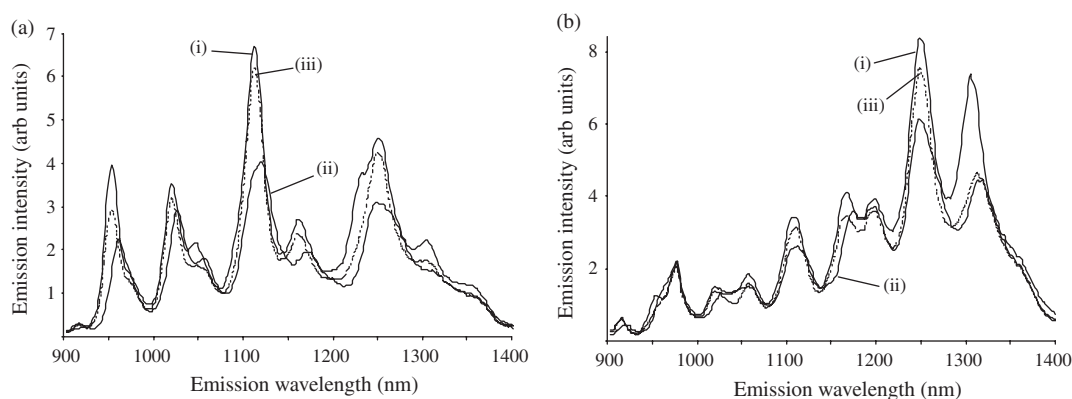


Fig. 7. The emission spectra of SDS-SWNTs from (a) 660 nm excitation and (b) 785 nm excitation. The (i) SDS-SWNTs, (ii) SDS-SWNTs quenched from Cd^{2+} , and (iii) recovered from EDTA treatment are shown.

contributions of 43 different fluorescing tubes. Deconvolution of the spectra shown in Fig. 5 gives the individual components for each SWNT n,m value. This suggests there is selectivity with regard to the quenching. There have been previous reports of selectivity with regard to those SWNTs with band gaps above/below threshold values [16], but this is clearly another phenomenon.

In attempts to understand this observation, we focus on two SWNTs with similar diameters and emission wavelengths. The 10,5 tube has a diameter of 1.050 nm and emits at 1252 nm, while the 8,7 tube is 1.032 nm in diameter and emits at 1270 nm. The difference between them is that 10,5 is a mod 2 tube while 8,7 is a mod 1 SWNT [17]. Given their similarities in electronic properties, it follows that they would be expected to exhibit similar fluorescence quenching in the presence of Cd^{2+} . Surprisingly, careful observation of Figs 5 and 6 shows that the two tubes act differently. It appears that the emission contribution of the 10,5 tube at 1252 nm is completely eliminated in the presence of Cd^{2+} while the 8,7 tube follows a decay similar to that found in SDBS quenching, i.e., the greater the metal concentration the greater the decrease in fluorescence. Upon further inspection, it appears that the emission of other mod 2 nanotubes also completely ceases in the presence of Group 12 metal ions while the mod 1 nanotubes follow a more normal diminishing of the fluorescence intensity. This apparent distinguishment between mod 1 and mod 2 should be very unlikely since there is no reason for there to be any difference, therefore there must be an alternative rationalization.

As was reported previously [2], transition metal ions formed aggregates with the surfactant however, no evidence for a similar precipitate is observed here. The bundling of SWNTs results in the loss of fluorescence intensity [18]. Adding 3.0 mM Cd^{2+} to the SDS-SWNTs causes a reduction in fluorescence (61% of its original intensity), Fig. 7. Subsequently adding ethylenediaminetetraacetic acid (EDTA) restores the fluorescence to 93% of its original intensity and shifts the peaks to their original position. Thus tight bundling is unlikely (see below). A similar effect was observed during CdS coating of SDS-solubilized SWNTs [3]. The fluorescence of the SDS-SWNTs was quenched in the presence of Cd^{2+} . Upon addition of the sulfur source (thiourea), formation of CdS removes the free Cd^{2+} and the fluorescence is regained. Furthermore, the apparent selectivity (or shift) observed during the addition of Cd^{2+} is overcome after the SWNTs are coated with CdS. It is possible that given the strong coordination of the Group 12 metals to the surfactant a bridging complex $\text{SWNT} \cdot \cdot \cdot \text{SDS} \cdot \text{M}^{2+} \cdot \text{SDS} \cdot \cdot \cdot \text{SWNT}$ could occur which would result in the close proximity of the SWNTs and hence quenching. However, cryogenic TEM did not show any evidence for such aggregates even with an excess of Group 12 metal salt.

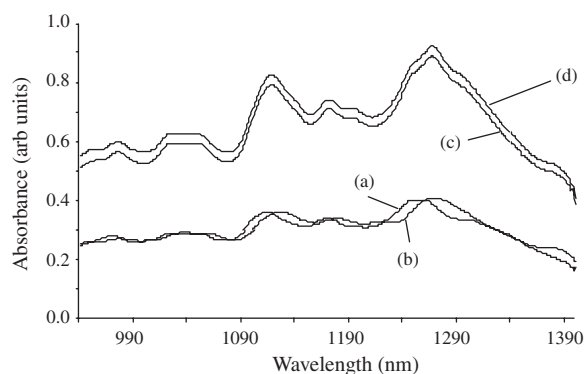


Fig. 8. The absorbance spectra of (a) SDS-SWNTs in H_2O and (b) SDS-SWNTs with Cd^{2+} . Shown for comparison are (c) SDBS-SWNTs in H_2O , and (d) SDBS-SWNTs with Cd^{2+} .

In the absence of detectable SWNT bundling and metal salt aggregation, the changes in fluorescence must be due to either a ground state or excited state process. To distinguish between the two possible mechanisms, we have looked at the absorption region of the nanotubes. As may be seen from Fig. 8, the absorbance spectra of SDBS-SWNTs remains unchanged upon the addition of Cd^{2+} , although the fluorescence is quenched. In contrast, the electronic structure of SDS-SWNTs is disrupted as indicated by the significant shift in the bands in the 900–1400 nm region. It should be noted that no shift in the absorption spectra is observed for either SDBS-SWNTs or SDS-SWNTs in the presence of Group 2 metal ions. Thus, even though the cadmium salts do not absorb at 660 or 785 nm, the presence of ions in solution affect the ground state of the SDS surfacted nanotubes, shifting their absorption energies. This seems contradictory, however, because the emission data we have obtained is due to excitation at 660 or 785 nm.

It is clear that the ground state of the SDS-SWNTs is altered in the presence of Group 12 metal ions. When the ground state is affected, we would expect the excitation wavelength for each individual n,m SWNT to change. To determine if this is occurring, the change in both excitation and emission wavelength for individual SWNTs can be probed by constructing a photoluminescence map as shown in Fig. 9 [19]. In considering the 10,5 and 8,7 SWNTs discussed above, the addition of 5 mM CdCl_2 to SDS-SWNTs results in a significant shift of the excitation wavelength of each SWNT. The resulting shift in the emission wavelengths are different for each n,m value, and thus, the apparent “selectivity” observed in the fluorescence spectra from 660 to 785 nm excitation is actually a result of different shifts in the emission spectrum that cannot be fitted using commercial software. The resulting combined peaks happen to look like there is selective quenching!

Careful observation of the spectra (Fig. 10) shows that the different chirality nanotube’s emission wavelengths are shifted by all metals but to varying degrees. This is expected, however, because the different chirality nanotubes have different electronic structures (bandgaps) and diameters. The plots of the emission wavelength shifts in relation to the bandgap (Fig. 11) and diameter of the SWNT are very similar. This is not surprising given the near inverse relationship between the diameter and bandgap. Both variables correlate well with the observed shifts, and the interdependency of the two makes it impossible to assign the effect to one variable or another.

With an understanding that the peaks in the fluorescence spectrum are shifted when Zn^{2+} , Cd^{2+} and Hg^{2+} are added, it is still possible to measure the intensity of 11 (n,m) values as a function of metal concentration. As may be seen from Fig. 12, the corrected decreases in fluorescence intensity of 4

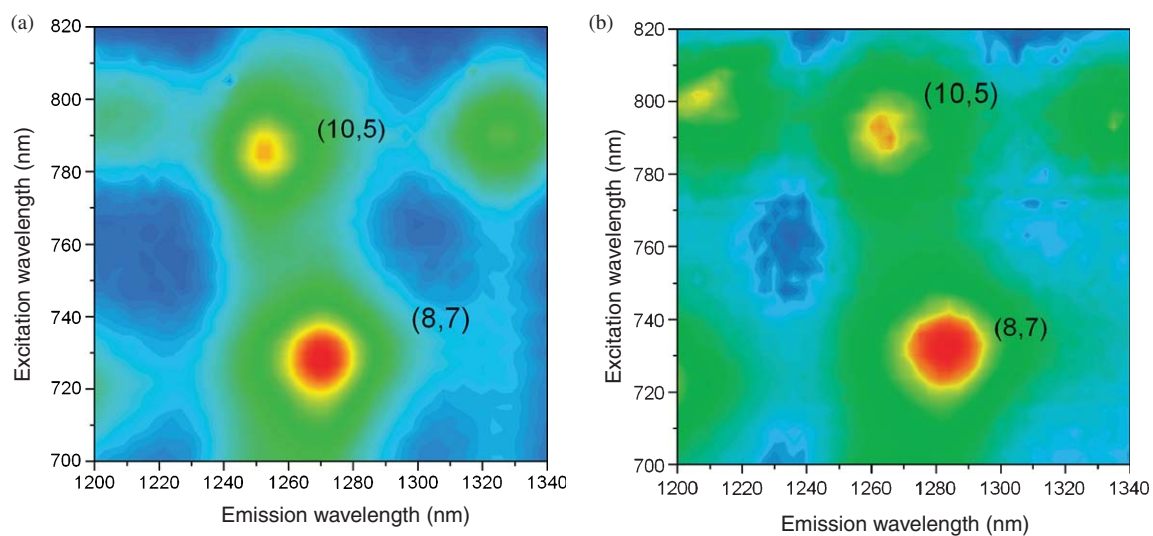


Fig. 9. The 2D excitation and emission plot of the 10,5 and 8,7 SWNTs for (a) SDS-SWNTs and (b) SDS-SWNTs in the presence of 5 mM CdCl₂.

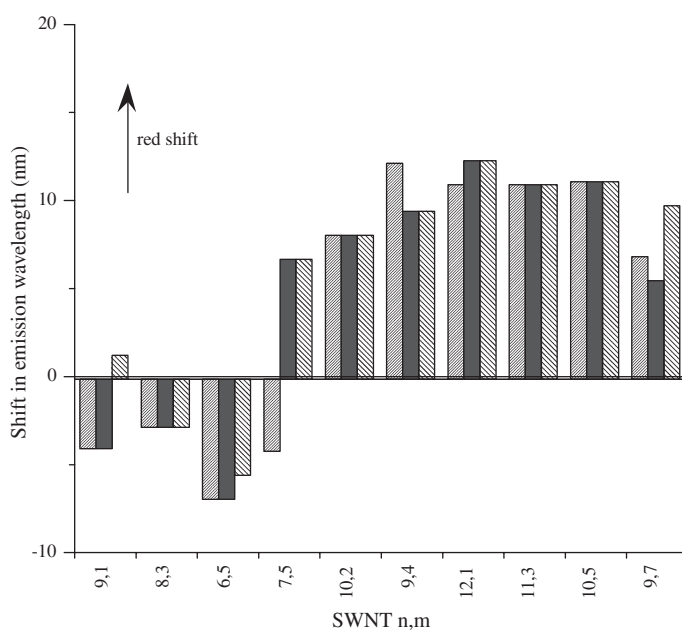


Fig. 10. Shift (red = +ve, blue = -ve) of the emission wavelength for selected SWNT n,m values for the addition of 5 mM of ZnCl₂ (▨), CdCl₂ (■), and HgCl₂ (▩) for 785 nm irradiation showing the dependence on both the SWNT, n,m and the metal cation.

representative nanotubes do not follow the trend expected from Stern-Volmer behavior. Instead there appears to be a critical concentration of metal ion, $[M^{2+}]_c$, that causes a steep change in fluorescence intensity. Above this concentration there appears to be no significant further reduction in fluorescence intensity. An important observation is that the critical concentration is not the same for each SWNT (n,m)

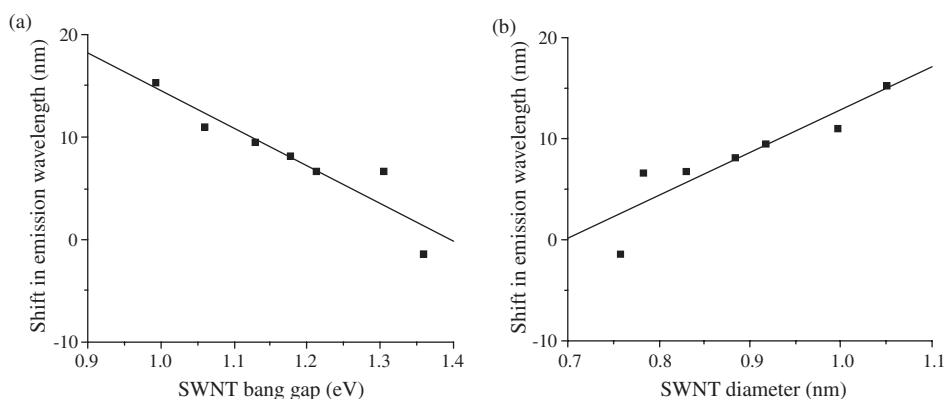


Fig. 11. Plot of shift in emission wavelength as a function of (a) SWNT band gap ($R^2=0.870$) and (b) SWNT diameter ($R^2=0.814$).

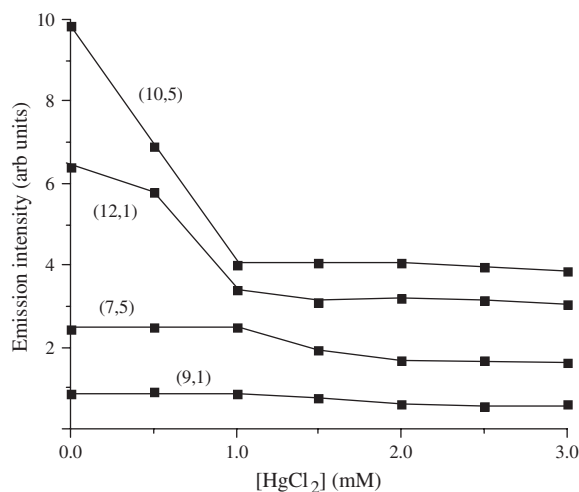


Fig. 12. Plot of fluorescence intensity as a function of concentration of HgCl₂ for selected SWNTs showing the dependence on the SWNT chirality of the step-change in fluorescence intensity. All intensities are corrected for shifts in the emission spectra.

value, i.e., it is chirality dependent. Notice in Fig. 12 that the 10,5 and 12,1 nanotubes have a critical concentration at 1.0 mM while the 7,5 nanotube is at 1.5 mM and the 9,1 tube is closer to 2.0 mM. To better assess this event, the critical concentration, ($[M^{2+}]_c$), was determined for each of the n,m nanotubes to determine if there were any trends present. There is no apparent relationship between the $[M^{2+}]_c$ and the band gap or the diameter of the SWNTs (Fig. 13). A distinct relationship between the identity of the metal ion and the critical concentration exists in Fig. 14. The general trend follows that $[Zn^{2+}]_c > [Cd^{2+}]_c > [Hg^{2+}]_c$ for a given n,m chirality nanotube.

In the absence of solution redox chemistry [20], previous examples of abrupt changes in fluorescence intensity that are not associated with SWNT bundling involve changes in the environment dielectric constant (electronic environment) or changes in the surfactant wrapping of the SWNT. The addition of acid to SWNT solutions reacts reversibly with preadsorbed oxygen to protonate the sidewalls of the SWNTs [21]. This change in dielectric constant bleaches the fluorescence of the nanotubes. DNA

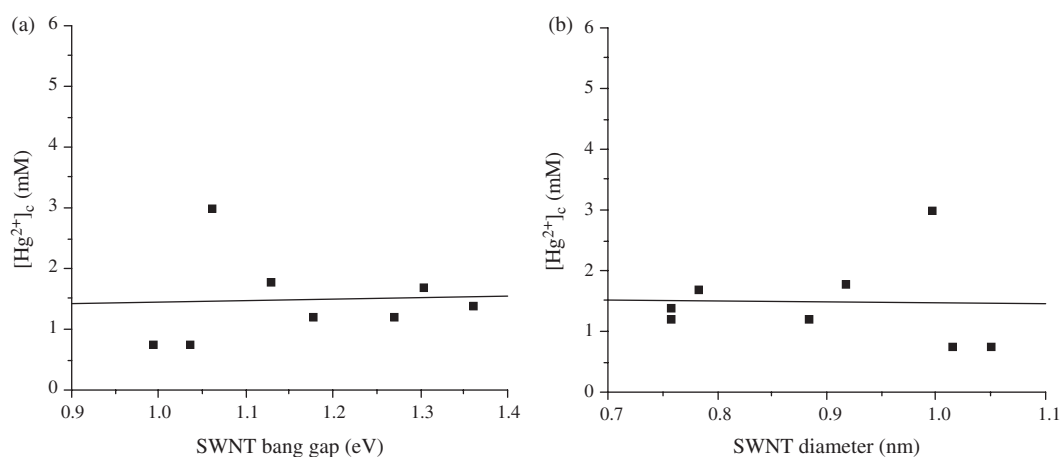


Fig. 13. Critical concentration of HgCl_2 as a function of (a) SWNT bang gap and (b) SWNT diameter.

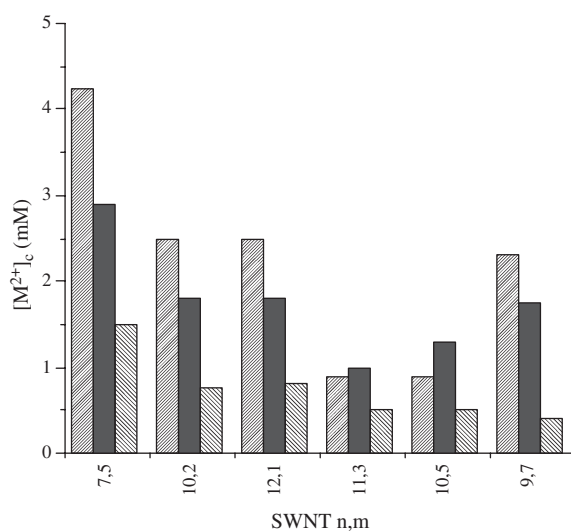


Fig. 14. Critical concentration of M^{2+} (mM) as a function of SWNT n,m value for ZnCl_2 (▨), CdCl_2 (■), and HgCl_2 (▩) for 785 nm irradiation.

wrapped SWNTs were shown to undergo a conformation change when exposed to HgCl_2 in solution [22]. The transition from a B configuration to a Z structure simultaneously caused an abrupt decrease in the fluorescence intensity due to the rearrangement of the surfactant around the nanotubes. This presumably also induced a change in the dielectric constant near the surface of the nanotube.

3.3. Surfactant · · SWNT versus surfactant · · M^{2+} interactions

For SDBS-surfacted SWNTs, the interaction of the metal ions with the surfactant ($\text{M}^{2+} \cdot \cdot \cdot \text{SDBS}$) is undoubtedly weaker than the interaction of the surfactant with the SWNT ($\text{SDBS} \cdot \cdot \cdot \text{SWNT}$). Thus, the addition of either Group 2 or 12 metals does not appear to alter the surfactant micellar structure around the SWNT. Instead, the fluorescence of the SWNTs is decreased due to the localized presence of the

metal ion's charge. In contrast, in the case of SDS, the interaction of the surfactant with the SWNT is limited by van der Waal interactions and the structure of the SDS-SWNT conjugate is readily overcome by the addition of the Group 12 metal but not by Group 2 metals. This differentiation can be rationalized by a consideration of the relative hardness of the metal ions and the sulfonate and sulfate "ligands".

Group 2 metals can be considered to be hard Lewis acids, will be mostly solvated in solution, and will form primarily ionic interactions with the surfactants. The closeness of the metal ion to the SWNT surface will solely depend on the surfactant · · SWNT interaction (Fig. 3). Group 12 metals will essentially form covalent bonds to the surfactants. With SDBS, this results in the forcing of the Group 12 metal ion close to the surface of the SWNT but without overcoming the π - π interactions between the SDBS and the SWNT surface. Based upon known crystal structure data for sulfonate and sulfate "ligands" complexes [23], we propose that the Group 12 metal ions will form strong covalent complexes with the surfactant, which with SDS causes a rearrangement of the surfactant · · SWNT conjugate structure. As the metal concentration reaches a critical level we propose it forces the restructuring of the micelle (Fig. 15). The rearrangement of the solvation environment around the SWNT results in a change in the dielectric constant around the SWNT. Further support for this surfactant rearrangement is evident in the lack of observed quenching. It follows that surfactant binding to the metal ion rearranges the surfactant and lifts the metal ion away from the surface of the nanotubes such that no quenching can occur. Thus, constant fluorescence intensity is achieved as observed in Fig. 12.

The general trend observed in Fig. 14 is in line with the size and relative coordinative ability of the metal ions causing disruption of the micelle. The small size of Zn^{2+} limits the number of surfactant head groups to which it can coordinate while the larger size of Hg^{2+} permits the disruption of more surfactant

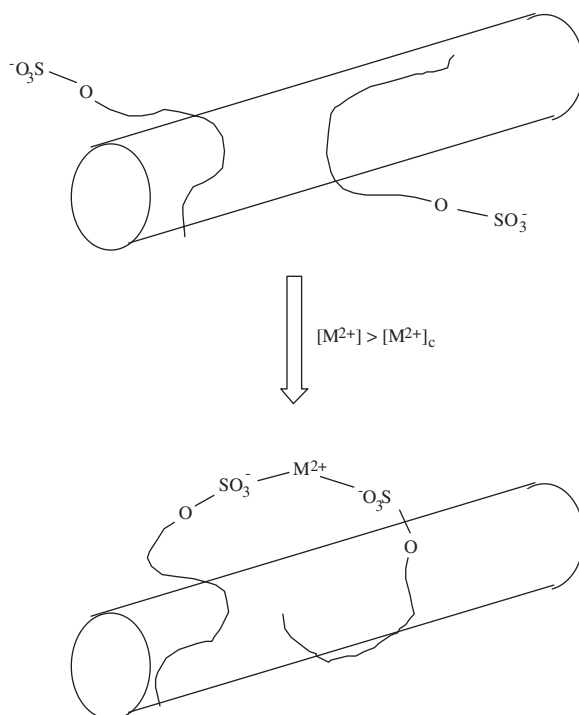


Fig. 15. Schematic representation of the reorganization of the SDS surfactant micellar structure around a SWNT promoted by the addition of a Group 12 metal ion.

molecules. Thus, it follows that the amount of Hg^{2+} needed to disrupt the same number of surfactant molecules as Zn^{2+} is less.

4. Conclusions

The solubilization of unfunctionalized SWNTs into aqueous solution is going to be increasingly important especially in regard to both biological and environmental issues [24]. It is therefore imperative to understand how various solubilization agents interact with the SWNT. Based upon the above results, we propose that an investigation of the quenching of fluorescence of anionic surfactant SWNTs by Group 2 metals allows for an indirect observation of the structure of the surfactant-SWNT conjugate. For example, the greater quenching (higher K_{sv}) observed for SDBS-SWNTs as compared to SDS-SWNTs is consistent with the metal being held closer to the SWNT surface; the ground state changes observed for SDS-SWNT conjugates are consistent with a rearrangement of the surfactant micelle. We propose that future studies on additional anionic surfactants will offer insight into both the structure and stability of surfactant-SWNT conjugates.

Acknowledgments

Financial support for this work is provided by the Robert A. Welch Foundation and the National Science Foundation (grant number EEC-0647452, CBEN).

References

- [1] J.J. Brege, C. Gallaway and A.R. Barron, Fluorescence quenching of single walled carbon nanotubes in SDBS surfactant suspension by metal ions: quenching efficiency as a function of metal and nanotube identity, *J Phys Chem C* **111** (2007), 17812–17820.
- [2] J.J. Brege, C. Gallaway and A.R. Barron, Fluorescence quenching of single walled carbon nanotubes with transition metal ions, *J Phys Chem C* **113** (2009), 4270–4276.
- [3] R. Loscutova and A.R. Barron, Coating single-walled carbon nanotubes with cadmium chalcogenides, *J Mater Chem* **15** (2005), 4346–4353.
- [4] V.C. Moore, M.S. Strano, E.H. Haroz, R.H. Hauge and R.E. Smalley, Individually suspended single-walled carbon nanotubes in various surfactants, *Nano Lett* **3** (2003), 1379–1382.
- [5] V.V. Didenko, V.C. Moore, D.S. Baskin and R.E. Smalley, Visualization of individual single-walled carbon nanotubes by fluorescent polymer wrapping, *Nano Lett* **5** (2005), 1563–1567.
- [6] P.K. Rai, A.N.G. Parra-Vasquez, J. Chattopadhyay, R.A. Pinnick, F. Liang, A.K. Sadana, R.H. Hauge, W.E. Billups and M. Pasquali, Dispersions of functionalized single-walled carbon nanotubes in strong acids: solubility and rheology, *J Nanosci Nanotechnol* **7** (2007), 3378–3385.
- [7] R.E. Anderson and A.R. Barron, Solubilization of single-wall carbon nanotubes in organic solvents without sidewall functionalization, *J Nanosci Nanotechnol* **7** (2007), 3436–3440.
- [8] J. Chattopadhyay, A.K. Sadana, F. Liang, J.M. Beach, Y. Xiao, R.H. Hauge and W.E. Billups, Carbon nanotube salts. arylation of single-wall carbon nanotubes, *Org Lett* **7** (2005), 4067–4069.
- [9] M.J. O'Connell, S.M. Bachilo, C.B. Huffman, V.C. Moore, M.S. Strano, E.H. Haroz, K.L. Rialon, P.J. Boul, W.H. Noon, C. Kittrell, J. Ma, R.H. Hauge, R.B. Weisman and R.E. Smalley, Band gap fluorescence from individual single-walled carbon nanotubes, *Science* **297** (2002), 593–596.
- [10] T.J. McDonald, C. Engtrakul, M. Jones, G. Rumbles and M.J. Heben, Kinetics of PL quenching during single-walled carbon nanotube rebundling and diameter-dependent surfactant interactions, *J Phys Chem B* **110** (2006), 25339–25346.
- [11] K. Yurekli, C.A. Mitchell and R. Krishnamoorti, Small-angle neutron scattering from surfactant-assisted aqueous dispersions of carbon nanotubes, *J Am Chem Soc* **126** (2004), 9902–9903.

- [12] H.-P. Hentze, S.R. Raghavan, C.A. McKelvey and E.W. Kaler, Silica hollow spheres by templating of cationic vesicles, *Langmuir* **19** (2003), 1069–1074.
- [13] E.A. Whitsitt and A.R. Barron, Effect of Surfactant on particle morphology for liquid phase deposition of submicron silica, *J Coll Interf Sci* **287** (2005), 318–325.
- [14] S. Niyogi, S. Boukhalfa, S.B. Chikkannanavar, T.J. McDonald, M.J. Heben and S.K. Doorn, Selective aggregation of single-walled carbon nanotubes via salt addition, *J Am Chem Soc* **129** (2007), 1898–1899.
- [15] H. Adams, C.A. Hunter, K.R. Lawson, J. Perkins, S.E. Spey, C.J. Urch and J.M. Sanderson, A supramolecular system for quantifying aromatic stacking interactions, *Chem Eur J* **7** (2001), 4863–4877.
- [16] M.J. O’Connell, E.E. Eibergen and S.K. Doorn, Chiral selectivity in the charge-transfer bleaching of single-walled carbon-nanotube spectra, *Nature Mater* **4** (2005), 412–418.
- [17] R.B. Weisman and S.M. Bachilo, Dependence of optical transition energies on structure for single-walled carbon nanotubes in aqueous suspension: an empirical kataura plot, *Nano Lett* **3** (2003), 1235–1238.
- [18] Y. Tan and D.E. Resasco, Dispersion of single-walled carbon nanotubes of narrow diameter distribution, *J Phys Chem B* **109** (2005), 14454–14460.
- [19] S.M. Bachilo, M.S. Strano, C. Kittrell, R.H. Hauge, R.E. Smalley and R.B. Weisman, Structure-assigned optical spectra of single-walled carbon nanotubes, *Science* **298** (2002), 2361–2366.
- [20] M. Zheng and B.A. Diner, Solution redox chemistry of carbon nanotubes, *J Am Chem Soc* **126** (2004), 15490–15494.
- [21] M.S. Strano, C.B. Huffman, V.C. Moore, M.J. O’Connell, E.H. Haroz, J. Hubbard, M. Miller, K. Rialon, C. Kittrell, S. Ramesh, R.H. Hauge, R.E. Smalley, Band-gap-selective protonation of single-walled carbon nanotubes in solution, *J Phys Chem B* **107** (2003), 6979–6985.
- [22] D.A. Heller, E.S. Jeng, T.-K. Yeung, B.M. Martinez, A.E. Moll, J.B. Gastala and M.S. Strano, Optical detection of DNA conformational polymorphism on single-walled carbon nanotubes, *Science* **311** (2006), 508–511.
- [23] A. Keys, T. Barbarich, S.G. Bott and A.R. Barron, Tert-butyl compounds of gallium, *J Chem Soc Dalton Trans* (2000), 577–588.
- [24] C.M. Sayes, F. Liang, J.L. Hudson, J. Mendez, W. Guob, J.M. Beach, V.C. Moore, C.D. Doyle, J.L. West, W.E. Billups, K.D. Ausman and V.L. Colvin, Functionalization density dependence of single-walled carbon nanotubes cytotoxicity in vitro, *Toxicol Lett* **161** (2006), 135–142.